

# Further observations of quasars in ESO/SERC field 927

Roger G. Clowes,<sup>1★†</sup> Luis E. Campusano<sup>2★</sup> and Matthew J. Graham<sup>1★‡</sup>

<sup>1</sup>*Centre for Astrophysics, University of Central Lancashire, Preston PR1 2HE*

<sup>2</sup>*Observatorio Astronómico Cerro Calán, Departamento de Astronomía, Universidad de Chile, Casilla 36-D, Santiago, Chile*

Accepted 1999 May 11. Received 1999 May 6; in original form 1999 March 3

## ABSTRACT

We present the spectra and redshifts of 62 quasars, from observations made with the Cerro Tololo Inter-American Observatory (CTIO) 4-m Blanco Telescope. These quasars form part of a total sample of 118 (with 56 having been published previously), which is being used for analysis of structure in the early universe. Quasars of particular interest are noted, including eight broad absorption line (BAL) quasars and two quasars with unusual emission spectra. Finally, we include a short summary of the present status of the large quasar group (LQG) that was discovered by Clowes & Campusano from the earlier observations. The quasars are from an area  $\sim 25.3 \text{ deg}^2$  of ESO/SERC field 927, which is centred at (1950)  $10^{\text{h}}40^{\text{m}}00^{\text{s}}$ ,  $05^{\circ}00'00''$ .

**Key words:** surveys – quasars: general – large-scale structure of Universe.

## 1 INTRODUCTION

This paper presents spectroscopic observations, with the Cerro Tololo Inter-American Observatory (CTIO) 4-m Blanco Telescope, of 62 quasars from a survey in ESO/SERC field 927. It supplements the paper of Clowes & Campusano (1994), which presented the observations of 56 quasars from the survey. The construction of this wide-angle, sparse sample, suitable for the analysis of structure in the early universe, is concluded here.

Field 927 is in the direction of the large quasar group (LQG) that was discovered by Clowes & Campusano (1991). The LQG has size  $\sim 100\text{--}200 h^{-1} \text{ Mpc}$  at  $z \sim 1.3$ , and was discovered from the 56 quasars in Clowes & Campusano (1994) together with five quasars from the survey for which redshifts were already known (Keable 1987). In 1991, 10 members of the LQG were known, together with three that were not from our survey. Following these later observations, 15 members are known, plus the extra three. A brief description of the current appearance of the LQG is given in this paper, but see Clowes, Campusano & Graham (1995) and Campusano, Clowes & Graham (in preparation) for more details.

The survey was by the method of Automated Quasar Detection (AQD – Clowes 1986; see also Clowes, Cooke & Beard 1984), in which an objective-prism plate is digitized by the COSMOS machine and candidates for quasars are selected by software. The plate was UJ5846P from the UK Schmidt Telescope; it is centred at (field 927, 1950)  $10^{\text{h}}40^{\text{m}}00^{\text{s}}$ ,  $05^{\circ}00'00''$ . Quasar candidates

were selected by emission lines or ultraviolet excess, from  $\sim 25.3 \text{ deg}^2$  of the plate.

166 high-grade quasar candidates were selected for spectroscopic follow-up. These candidates, which must all show at least one emission line in the objective-prism spectra, were sorted in descending order of an AQD line-strength parameter (LSP: total line energy for the principal line/total continuum energy), with a cut-off at  $\text{LSP} \sim 0.014$ . The first 80 candidates to be observed with slit spectroscopy were chosen from two bands at the top and the bottom of the ordered list so that both strong-lined (S-band) and weak-lined (W-band) candidates were included. This first observing campaign confirmed 56 quasars (Clowes & Campusano 1994). The candidates were observed at random with respect to magnitude and position on the sky.

In this paper we report the observations of the remaining 86 candidates from the ordered list, most of them having AQD LSPs intermediate between the original strong- and weak-lined definitions. 62 of these candidates were confirmed as quasars. Here we present their spectra, redshifts, equivalent widths of the principal lines,  $B_j$  magnitudes, and comments for the quasars of particular interest.

## 2 OBSERVATIONAL DETAILS

Spectroscopic observations of the 86 quasar candidates were obtained on the nights of 1992 March 3/4–4/5, 1993 February 23/24–25/26, and 1994 February 7/8–10/11. All observations were with the CTIO 4-m Blanco Telescope and its Ritchey–Chrétien spectrograph. A summary of the instrumental configurations is given in Table 1.

Note that the Reticon CCD gave a wavelength coverage of

\* Visiting Astronomer at Cerro Tololo Inter-American Observatory.

† r.g.clowes@uclan.ac.uk

‡ Present address: Astrophysics Group, Blackett Laboratory, Imperial College, London, SW7 2BZ.

**Table 1.** A summary of the instrumental configurations for the observations with the CTIO 4-m Blanco Telescope and the Ritchey–Chrétien spectrograph. The columns are as follows: date of the observations; detector (CCD); gain; collimator/camera; grating; pixels; pixel size; pixel scale along the slit; dispersion; wavelength range.

Date	Detector (CCD)	Gain eADU <sup>-1</sup>	Col./Cam.	Grating	Pixels	Size μm	Scale arcsec pixel <sup>-1</sup>	Disp. Å pixel <sup>-1</sup>	Δλ Å
1992 Mar 03/04–04/05	Reticon II	1.1	Blue/BAS	KPGL–2	1200 × 400	27	0.88	3.60	3140–7420
1993 Feb 23/24–25/26	Tek 1024 # 2	1.1	Blue/FS	KPGL–2	1024 × 420	24	0.79	3.23	3266–6575
1994 Feb 07/08–10/11	Reticon II	0.98	Blue/BAS	KPGL–2	1200 × 400	27	0.88	3.60	3140–7420

Notes:

BAS: Blue Air Schmidt camera.

FS: Folded Schmidt camera.

Grating KPGL-2 is blazed at 4400 Å.

~3140–7420 Å for the 1992 and 1994 observations, while the Tek CCD, with fewer, smaller pixels in the dispersion direction, gave a reduced wavelength coverage of ~3266–6575 Å for the 1993 observations.

The main purposes of the observations of the quasar candidates were to establish, for as many as possible, their identities as quasars or stars and to measure redshifts. Integration times were therefore typically set to give signal-to-noise ratios for the continuum that are adequate (~8) rather than unnecessarily high. In some cases the signal-to-noise ratio that resulted was ~4, which can lead to increased errors for the redshifts. The width of the slit was 2 arcsec, which corresponds to spectral resolution ~10 Å. All of the candidates were observed with the long axis of the slit aligned approximately with the direction of atmospheric dispersion (i.e. the parallactic angle), and most with air-masses smaller than 2. The seeing was typically ~1.5 arcsec for the 1992 and 1994 observations and ≤1.5 arcsec for the 1993 observations. Photometric conditions were good on all occasions.

For the comparison arcs (He–Ar and Ne simultaneously), long and short integrations were taken at the beginning or end of each night, with the telescope in the meridian at  $\delta = 5^\circ$ . Further short arcs, to specify zero-point shifts, were taken regularly throughout each night, but not after each object integration. Previous experience (see Clowes & Campusano 1994) had shown that, when all the objects are in the same field, the time spent on object integrations could be increased by thus reducing the frequency of these short arcs. Any intervening zero-point shifts could be adequately specified by the night-sky emission lines.

The combination of the long arcs (to emphasize faint lines) and the short arcs generated the basic wavelength calibrations, requiring only zero-point shifts for individual objects. These reference arcs were fitted with a fifth-order polynomial function (i.e. six coefficients), giving rms deviations of ~0.5 Å for the conversion from pixels to wavelengths. The identified arc lines at the extremes of the spectral range had wavelengths 3187.74, 7311.72 Å for the 1992 and 1994 observations, and 3293.7, 6532.88 Å for the 1993 observations. The shifts in zero-point throughout each night were generally ≤3 pixel.

Spectrophotometric standards for the calibration of flux density were observed through a wide, 6.6-arcsec, slit and also a 2-arcsec slit. Typically, the sensitivity functions through the two slit widths differed only by 5–10 per cent. Consequently, the sensitivity functions for the 2-arcsec slit have been applied to the quasars without correction. The standard stars were EG 274, L745-46A, LTT 2415, LTT 3218, LTT 3864, LTT 4364, LTT 4816 and LTT 6248 from the list of Stone & Baldwin (1983). Standard figures for CTIO were used to correct for the atmospheric extinction.

A series of bias frames was taken for each night. Series of dome

flats and ‘projector’ flats were also taken for each night, for both the 2-arcsec and the 6.6-arcsec slit widths. Projector flats use a quartz projector lamp that is mounted inside the spectrograph, together with appropriate filters (Corning 9863, CuSO<sub>4</sub> and neutral density). The projector flats are needed because dome flats alone give too few counts for wavelengths below ~4000 Å. The final flats were constructed from the dome and projector flats, using an area in common for matching.

The processing of the data was done with IRAF, in part using the CTIO facilities.

### 3 CONFIRMED QUASARS

Table 2 summarizes the observations of the 62 survey candidates that were confirmed as quasars. The columns are as follows: the RA and Dec. for equinoxes 1950.0 and 2000.0; the date of the observation; the integration time in s; the AQD line-strength parameter (LSP) and band (‘S’ for strong-lined and ‘W’ for weak-lined); the  $B_J$  magnitude; the redshift; the equivalent width in Å and the identity (see the key at the end of the table) of the strongest emission line seen in the spectrum; comments. The quasars may be easily identified in the Digital Sky Survey, because the RA and Dec. are accurate to ~1 arcsec.

The spectra of these quasars are shown in Fig. 1. The spectra have been lightly smoothed by a Gaussian distribution with a  $\sigma = 1.0$  pixel to enhance the visibility of features in these small plots. Note that five of the 62 quasars already had redshifts, but not published spectra, from Keable (1987). One of the Keable (1987) redshifts was wrong; see Table 2 and the notes on individual quasars.

Wavelengths and equivalent widths of emission lines were measured with IRAF, using, in most cases, the unsmoothed and smoothed spectra respectively. The wavelengths of emission lines have been measured from the peaks when they are well-defined and otherwise from estimates of the centroids. Two quasars, noted in the column for comments in Table 2, have redshifts estimated from a single line, which was assumed to be Ly $\alpha$   $\lambda$ 1216.

The comment ‘imprecise  $z$ ’ means that the redshifts obtained from the different lines in a spectrum are not in good agreement (variations ~0.02). In some cases the relatively poor matching of lines appears to be intrinsic to the quasars. In other cases, contributing factors include Ly $\alpha$   $\lambda$ 1216 and N v  $\lambda$ 1240 not being resolved, emission lines affected by absorption, squat or asymmetric line profiles and low signal-to-noise ratio.

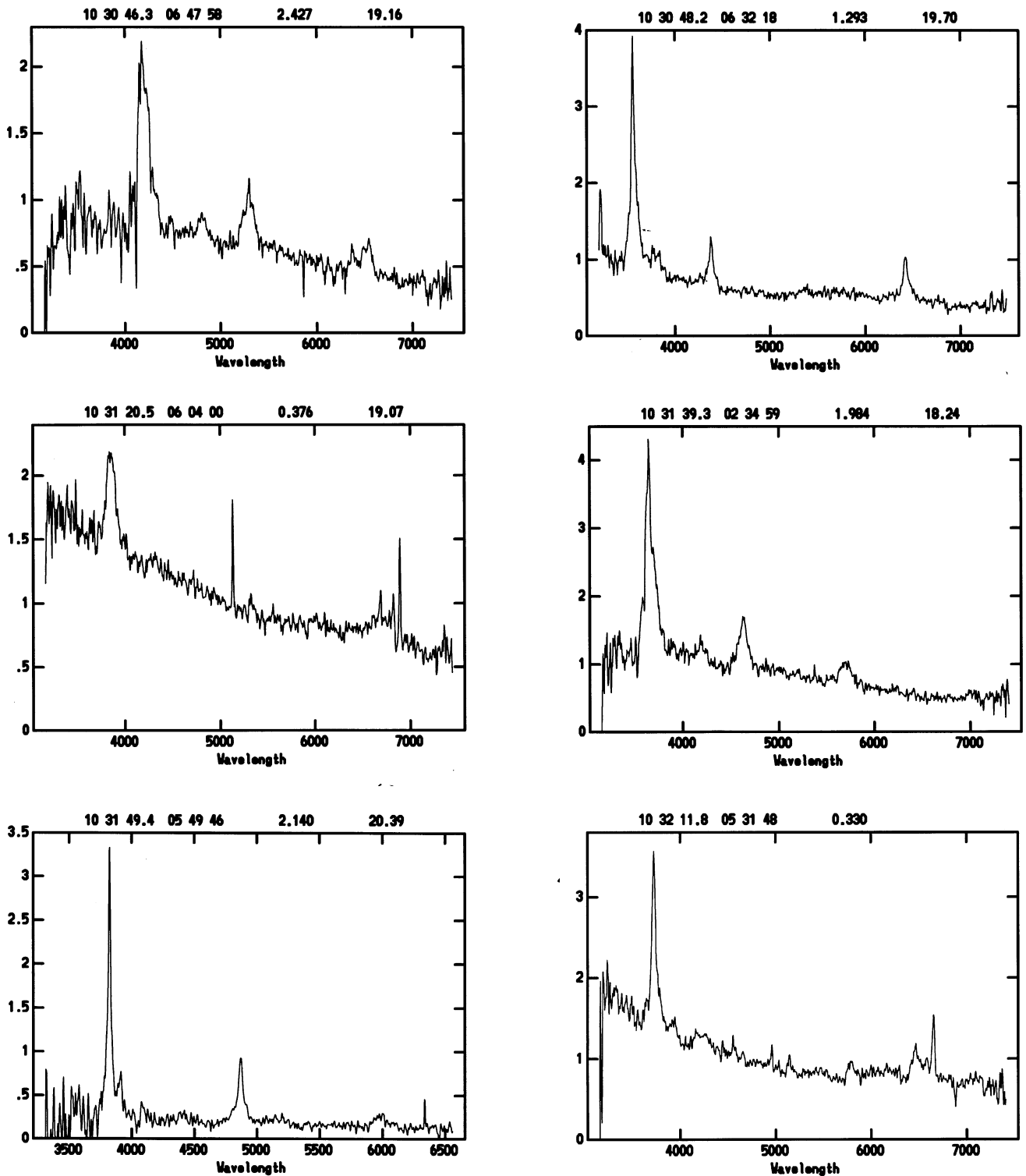
#### 3.1 Notes on individual quasars

The quasars in the following notes are identified by their 1950

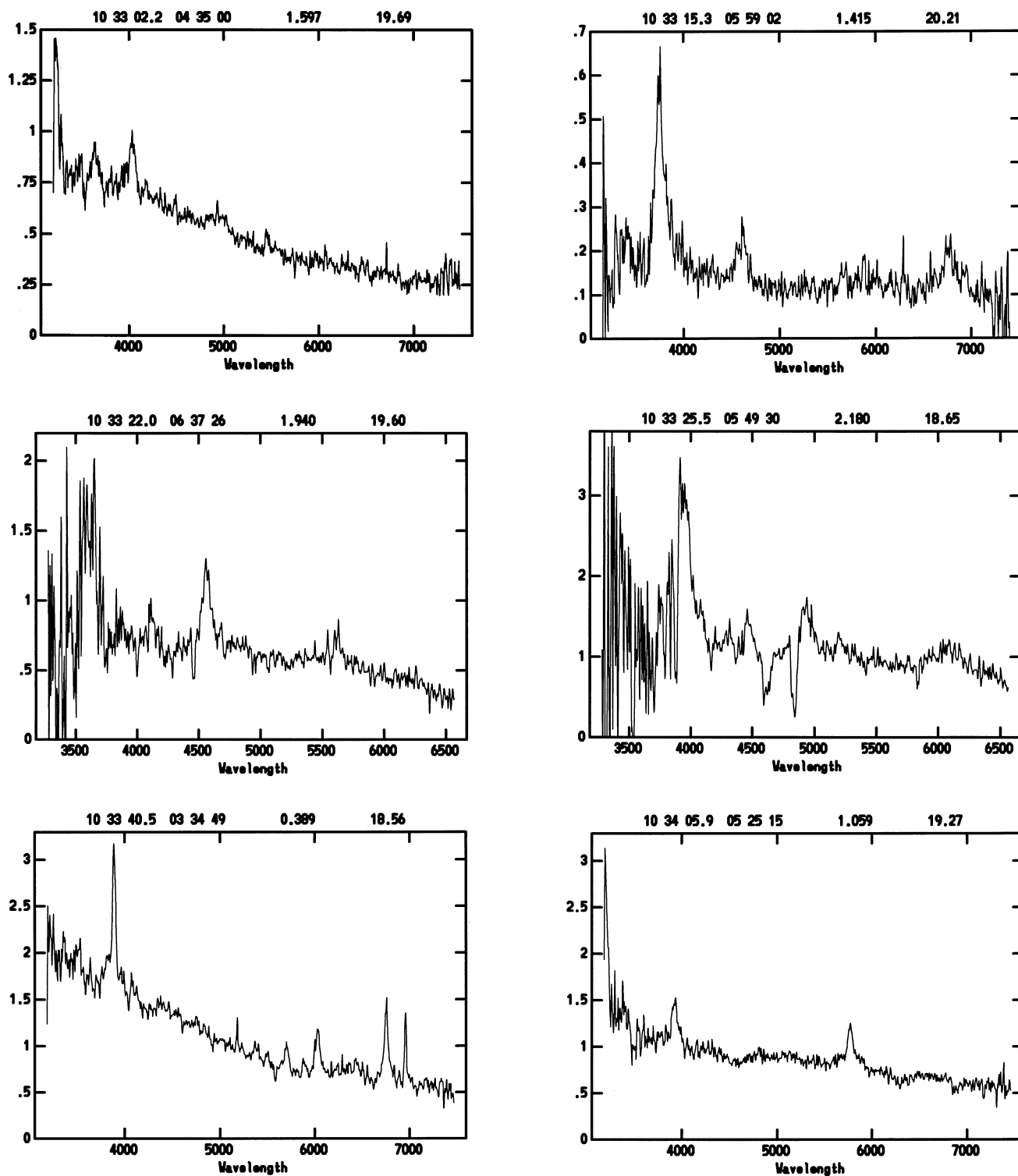
**Table 2.** Summary of observations. The columns are as follows: RA, Dec. (1950); RA, Dec. (2000); date of the observation; integration time in s; AQD line-strength parameter (LSP) and band ('S' for strong-lined, 'W' for weak-lined);  $B_J$  magnitude; redshift; equivalent width in Å (and identity of the strongest emission line: see footnote); comments.

RA, Dec (1950)	RA, Dec (2000)	Date	Int	LSP/Band	$B_J$	$z$	EW	Comments
10 30 46.3 06 47 58	10 33 23.0 06 32 29	1992 Mar 04/05	600	0.0600	19.16	2.427	251 (1)	
10 30 48.2 06 32 18	10 33 24.8 06 16 49	1994 Feb 07/08	900	0.0771	19.70	1.293	162 (2)	
10 31 20.5 06 04 00	10 33 56.8 05 48 30	1994 Feb 07/08	900	0.0760	19.07	0.376	67 (4)	
10 31 39.3 02 34 59	10 34 14.1 02 19 28	1992 Mar 04/05	300	0.0576	18.24	1.984	269 (1)	
10 31 49.4 05 49 46	10 34 25.6 05 34 15	1993 Feb 23/24	900	0.1444 S	20.39	2.140	711 (1)	
10 32 11.8 05 31 48	10 34 47.9 05 16 16	1992 Mar 03/04	900	0.0393 W		0.330	86 (4)	
10 33 02.2 04 35 00	10 35 37.8 04 19 27	1994 Feb 07/08	1200	0.0638	19.69	1.597	56 (1)	
10 33 15.3 05 59 02	10 35 51.5 05 43 29	1992 Mar 03/04	900	0.0485 W	20.21	1.415	257 (2)	
10 33 22.0 06 37 26	10 35 58.5 06 21 52	1993 Feb 23/24	400	0.0825 S	19.60	1.940	206 (1)	abs.
10 33 25.5 05 49 30	10 36 01.7 05 33 56	1993 Feb 24/25	300	0.0755	18.65	2.180	313 (1)	BAL; imprecise $z$
10 33 40.5 03 34 49	10 36 15.7 03 19 15	1994 Feb 08/09	900	0.0472 W	18.56	0.389	75 (5)	also Keable (1987, wrong $z$ )
10 34 05.9 05 25 15	10 36 41.9 05 09 40	1994 Feb 08/09	900	0.0228 W	19.27	1.059	72 (4)	also Keable (1987)
10 34 14.8 07 12 24	10 36 51.5 06 56 49	1992 Mar 04/05	600	0.0562	19.18	1.055	74 (3)	
10 34 41.6 06 34 54	10 37 18.1 06 19 18	1992 Mar 03/04	900	0.0554	19.57	1.997	152 (1)	BAL; imprecise $z$
10 34 53.8 04 52 51	10 37 29.5 04 37 15	1992 Mar 04/05	600	0.0652	19.53	1.826	228 (1)	
10 35 12.9 04 18 17	10 37 48.4 04 02 41	1993 Feb 24/25	400	0.0362 W	17.82	1.084	93 (3)	also Keable (1987)
10 36 00.4 06 45 26	10 38 36.9 06 29 48	1994 Feb 07/08	1200	0.0750	20.07	1.899	302 (1)	abs.; imprecise $z$
10 36 04.0 05 40 56	10 38 40.0 05 25 18	1994 Feb 08/09	1200	0.0743	19.78	1.070	>143 (2)	
10 36 55.9 03 53 15	10 39 31.2 03 37 36	1993 Feb 24/25	600	0.0701	19.85	1.914	429 (1)	
10 37 03.7 07 04 27	10 39 40.3 06 48 48	1992 Mar 04/05	600	0.0585	19.89	2.341	261 (1)	BAL?
10 38 13.2 04 32 13	10 40 48.7 04 16 32	1994 Feb 08/09	2400	0.0564	20.26	1.587	60 (1)	BAL? imprecise $z$
10 38 15.6 06 26 16	10 40 51.9 06 10 35	1993 Feb 23/24	500	0.0796	19.91	2.452	201 (1)	
10 38 16.5 02 56 56	10 40 51.4 02 41 15	1993 Feb 23/24	600	0.0798	19.96	1.989	216 (1)	imprecise $z$
10 38 32.2 03 46 31	10 41 07.4 03 30 49	1992 Mar 04/05	600	0.0580	19.36	1.686	308 (1)	
10 39 13.4 06 59 19	10 41 49.9 06 43 36	1992 Mar 03/04	600	0.0550	19.67	1.317	68 (2)	narrow lines
10 39 18.4 03 50 03	10 41 53.6 03 34 20	1993 Feb 24/25	500	0.0711		1.558	62 (3)	
10 39 35.5 03 59 49	10 42 10.8 03 44 06	1992 Mar 04/05	600	0.0564	19.78	1.007	61 (3)	
10 39 37.3 06 35 25	10 42 13.6 06 19 42	1992 Mar 04/05	600	0.0580	19.24	1.557	103 (2)	BAL
10 39 44.6 02 34 06	10 42 19.3 02 18 23	1993 Feb 24/25	700	0.0697	20.14	1.739	226 (1)	
10 40 03.5 05 32 28	10 42 39.4 05 16 44	1992 Mar 03/04	500	0.0535	19.40	1.868	267 (1)	
10 40 08.1 02 38 42	10 42 42.8 02 22 58	1992 Mar 04/05	600	0.0672	19.92	1.581	68 (2)	
10 40 40.6 05 45 31	10 43 16.5 05 29 46	1992 Mar 04/05	900	0.0578	20.34	1.260	61 (2)	
10 40 49.4 05 57 14	10 43 25.4 05 41 29	1993 Feb 23/24	600	0.0916 S	19.88	1.894	236 (1)	
10 40 53.8 02 46 59	10 43 28.6 02 31 14	1992 Mar 04/05	900	0.0558	19.74	2.546	252 (1)	BAL
10 41 08.2 06 40 03	10 43 44.5 06 24 18	1992 Mar 04/05	600	0.0645	20.02	2.136	309 (1)	narrow lines
10 41 45.6 04 45 35	10 44 21.1 04 29 49	1994 Feb 07/08	1200	0.0720	19.89	1.408	76 (2)	
10 41 55.9 06 33 17	10 44 32.1 06 17 31	1993 Feb 23/24	900	0.1239 S	19.96	2.147	211 (1)	
10 43 10.0 05 39 43	10 45 45.8 05 23 55	1992 Mar 03/04	600	0.0350 W		2.622?	160 (1)	single-line $z$ ; abs
10 43 16.5 06 40 24	10 45 52.7 06 24 36	1993 Feb 24/25	400	0.0326 W	17.88	1.506	62 (2)	also Keable (1987)
10 43 24.2 03 58 57	10 45 59.4 03 43 08	1992 Mar 04/05	600	0.0586	19.14	1.501	56 (2)	
10 44 07.0 05 46 56	10 46 42.9 05 31 06	1994 Feb 07/08	900	0.0678	19.18	2.682	190 (1)	single-line $z$ ; no C IV; abs
10 45 18.9 04 54 30	10 47 54.4 04 38 39	1993 Feb 23/24	500	0.0776	19.75	2.042	213 (1)	
10 45 42.5 06 35 33	10 48 18.6 06 19 41	1992 Mar 03/04	600	0.0344 W		0.404	44 (4)	
10 46 04.4 06 15 04	10 48 40.4 05 59 12	1993 Feb 23/24	500	0.0836 S	19.56	1.499	89 (2)	
10 46 56.6 05 21 24	10 49 32.2 05 05 31	1994 Feb 08/09	900	0.0421 W	19.37	1.113	174 (2)	also Keable (1987)
10 47 32.5 04 52 53	10 50 07.9 04 36 59	1994 Feb 07/08	900	0.0719	19.78	1.128	118 (2)	
10 48 02.1 03 35 40	10 50 37.1 03 19 45	1994 Feb 07/08	900	0.0846 S	19.66	1.904	218 (1)	imprecise $z$
10 48 14.9 03 48 14	10 50 49.9 03 32 19	1993 Feb 23/24	500	0.0780	19.69	2.171	216 (1)	imprecise $z$
10 48 26.8 04 05 46	10 51 01.9 03 49 51	1992 Mar 03/04	900	0.0483 W	19.74	0.865	43 (3)	
10 48 42.9 05 49 27	10 51 18.7 05 33 31	1992 Mar 04/05	600	0.0556	19.61	1.483	56 (2)	
10 48 50.2 06 53 34	10 51 26.3 06 37 38	1994 Feb 07/08	1200	0.0716	19.93	1.317	48 (3)	BAL
10 48 51.9 03 21 33	10 51 26.8 03 05 37	1992 Mar 04/05	300	0.0594	18.88	1.463	96 (4)	BAL
10 49 17.4 07 09 05	10 51 53.6 06 53 08	1994 Feb 07/08	600	0.0770	19.65	2.060	182 (1)	imprecise $z$
10 49 28.0 04 57 43	10 52 03.4 04 41 46	1992 Mar 03/04	900	0.0334 W		1.303	68 (2)	spectra added
		1992 Mar 04/05	1200				2100s	
10 49 30.9 04 14 26	10 52 06.1 03 58 29	1992 Mar 04/05	600	0.0655		1.457	130 (2)	
10 49 48.1 03 54 16	10 52 23.2 03 38 19	1993 Feb 24/25	600	0.0766		2.096	176 (1)	abs; imprecise $z$
10 50 08.4 05 42 19	10 52 44.1 05 26 21	1992 Mar 03/04	600	0.0403 W		1.521	60 (4)	abs; imprecise $z$
10 50 19.9 06 38 20	10 52 55.9 06 22 22	1992 Mar 03/04	600	0.0492 W		1.775	282 (1)	
10 50 35.2 05 12 22	10 53 10.7 04 56 24	1992 Mar 04/05	600	0.0582		2.530	278 (1)	imprecise $z$
10 50 48.1 05 19 22	10 53 23.6 05 03 23	1993 Feb 23/24	300	0.0886 S		2.275	203 (1)	abs; imprecise $z$
10 51 17.3 05 16 42	10 53 52.8 05 00 43	1992 Mar 04/05	300	0.0657		1.130	92 (2)	
10 51 21.5 06 44 44	10 53 57.5 06 28 45	1993 Feb 23/24	600	0.1021 S		2.788	218 (1)	abs; imprecise $z$

Identification of strongest emission lines: (1) Ly $\alpha$   $\lambda$ 1216+N v  $\lambda$ 1240; (2) C IV  $\lambda$ 1549; (3) C III]  $\lambda$ 1909; (4) Mg II  $\lambda$ 2798; (5) H $\beta$   $\lambda$ 4861.



**Figure 1.** The spectra of the quasars, obtained with the Ritchey–Chrétien spectrograph at the CTIO 4-m telescope. Each plot is of flux density  $f_\lambda$  against wavelength  $\lambda$  in  $\text{\AA}$ . The top labels are RA, Dec. (1950), redshift and  $B_J$  magnitude. The spectra have been lightly smoothed by a Gaussian distribution with  $\sigma = 1.0$  pixel to enhance the visibility of features in these small plots. The flux densities are in units of  $10^{-19} \text{W m}^{-2} \text{\AA}^{-1}$  or  $10^{-16} \text{erg s}^{-1} \text{cm}^{-2} \text{\AA}^{-1}$ , but note that the errors in the flux-density calibration will be  $\sim 10$ – $20$  per cent. Also, cosmic rays and remnants of the [O I]  $\lambda$  5577- $\text{\AA}$  night-sky line have been replaced by small horizontal sections.

Figure 1 – *continued*

coordinates. In these notes O VI refers to O VI  $\lambda$  1034, Ly $\alpha$  to Ly $\alpha$   $\lambda$  1216, N V to N V  $\lambda$  1240, Si IV + O IV to Si IV + O IV  $\lambda$  1400, C IV to C IV  $\lambda$  1549, C III] to C III]  $\lambda$  1909, Mg II to Mg II  $\lambda$  2798, and H $\beta$  to H $\beta$   $\lambda$  4861. All references are to emission lines unless explicitly qualified as absorption.

**10 33 22.0 06 37 26.** There are two absorption lines shortward

of C IV at 4459.5 and 4285.2 Å; the redshifts are, assuming C IV, 1.879 and 1.766. The emission redshift is 1.940. There is one absorption line shortward of Si IV + O IV at 3999.0 Å; the redshift is, assuming Si IV + O IV, 1.856 or, assuming C IV, 1.582. Thus, no redshift system is apparent. The absorption lines, although moderately wide (FWHM  $\sim$  25 and 20 Å for the lines at 4459.5 and 3999.0), do not appear to be broad absorption lines (BAL).

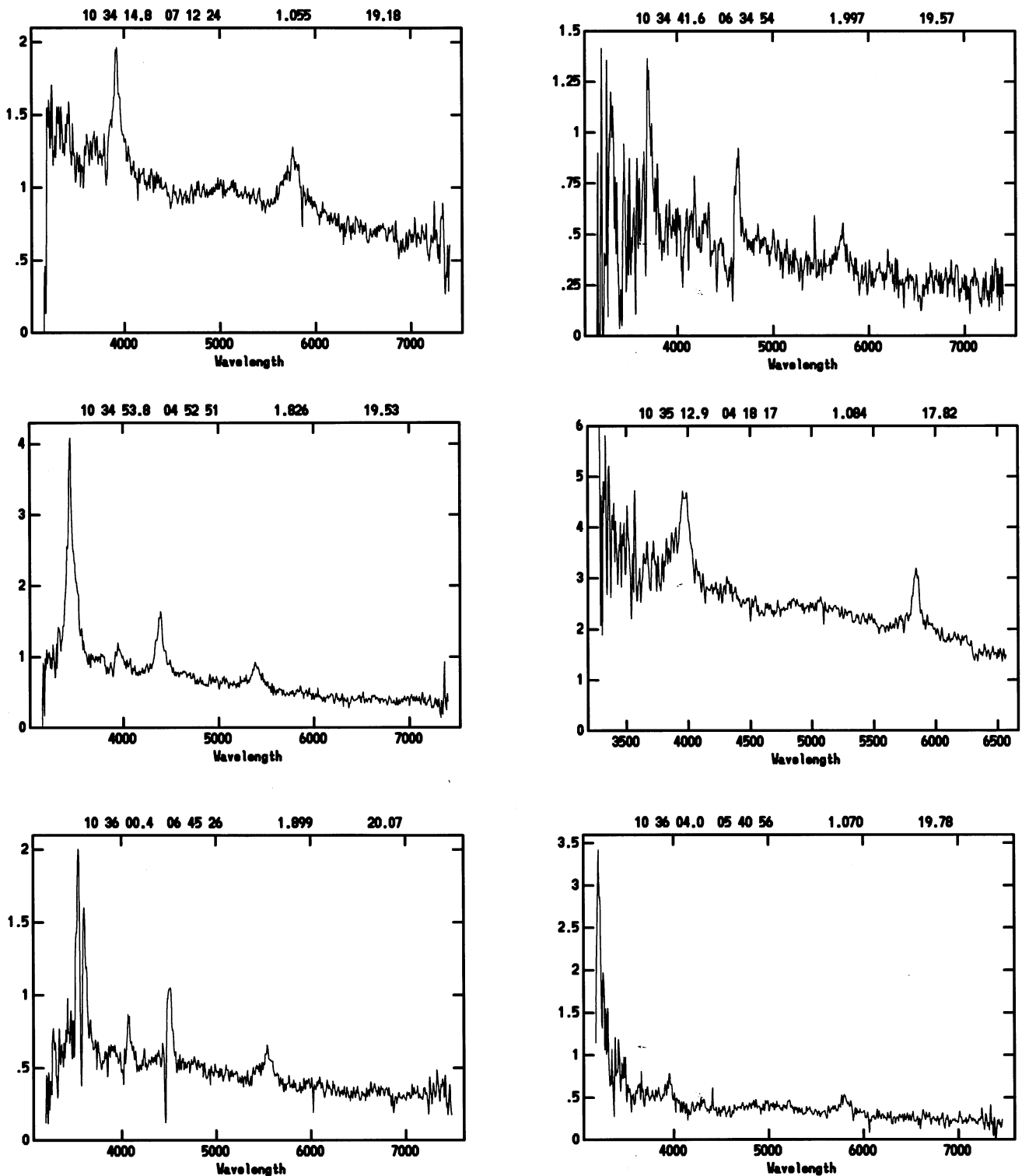


Figure 1 – continued

**10 33 25.5 05 49 30.** This is a BAL quasar. The characteristic broad and deep absorption lines, or troughs, of BAL quasars indicate the outflow from the quasar of absorbing matter at speeds of a few per cent of the speed of light. The speed of outflow is given by

$$v/c = \frac{\{(1 + z_{\text{em}})^2 - (1 + z_{\text{abs}})^2\}}{\{(1 + z_{\text{em}})^2 + (1 + z_{\text{abs}})^2\}}.$$

There are two prominent BAL troughs shortward of C IV at 4835.7 and 4616.4 Å, corresponding to redshifts 2.122 and 1.980. The emission redshift is 2.180, although the measurement is imprecise because of the absorption. The outflow speeds for these two troughs are then  $v/c \sim 0.018$  ( $5500 \text{ km s}^{-1}$ ) and  $v/c \sim 0.065$  ( $19460 \text{ km s}^{-1}$ ).

There is weak absorption shortward of Si IV + O IV at 4367.7 Å,

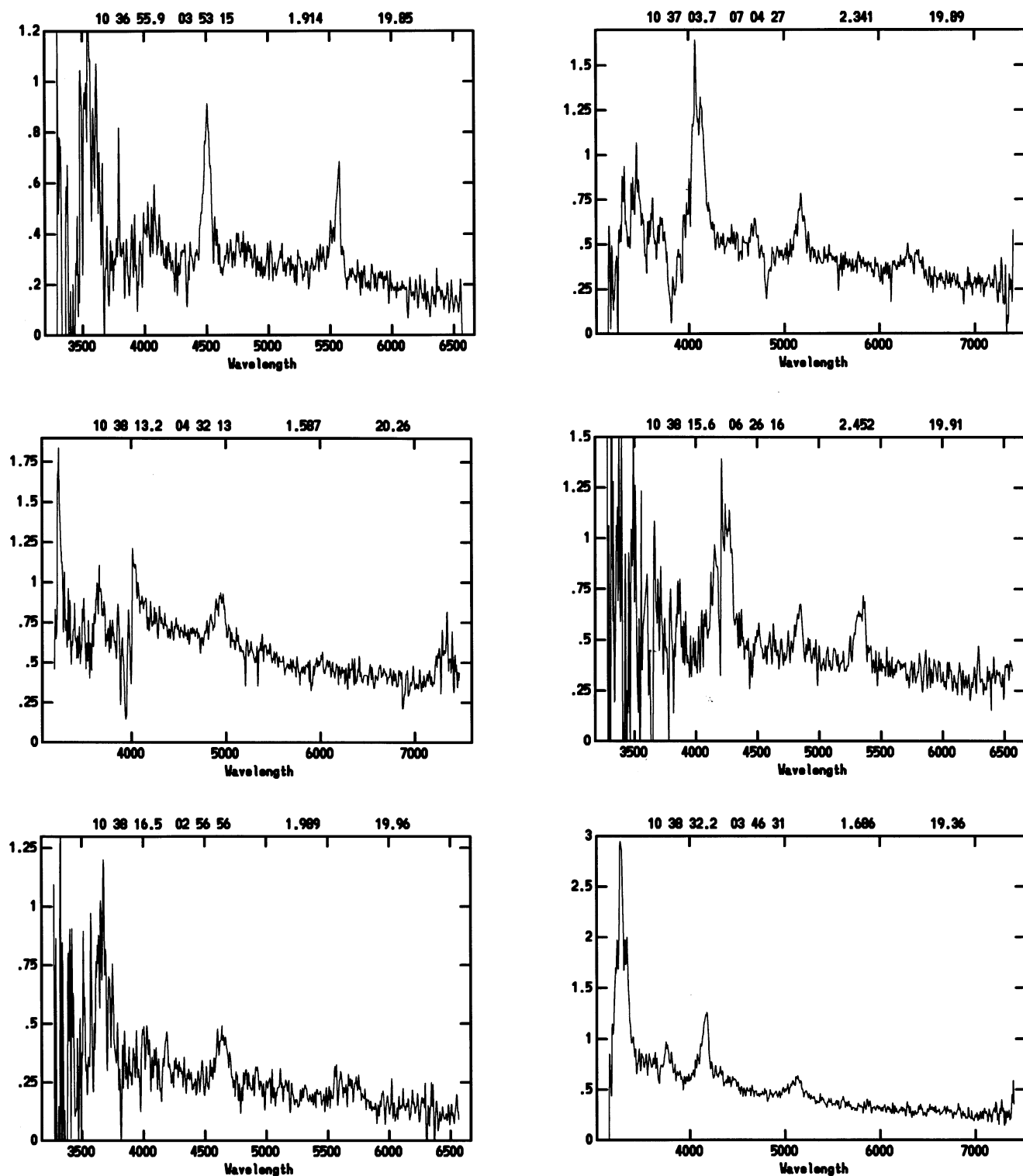


Figure 1 – continued

corresponding to redshift 2.120. This is probably the counterpart of the C IV absorption.

The signal-to-noise ratio is low shortward of Ly $\alpha$  + N v. One clear absorption feature is at 3878.2 Å, which could be Ly $\alpha$  at redshift 2.189 (unlikely) or N v at 2.128.

**10 33 40.5 03 34 49.** The redshift given by Keable (1987)

( $z = 1.513$ ) is wrong. Our observation of this quasar gives the redshift, unambiguously, as  $z = 0.389$ .

**10 34 41.6 06 34 54.** This is a BAL quasar. The signal-to-noise ratio in the region of the troughs is quite low, but the impression is that the whole region between Ly $\alpha$  + N v and C IV might be affected. There is a distinct trough shortward of C IV at 4528.3 Å

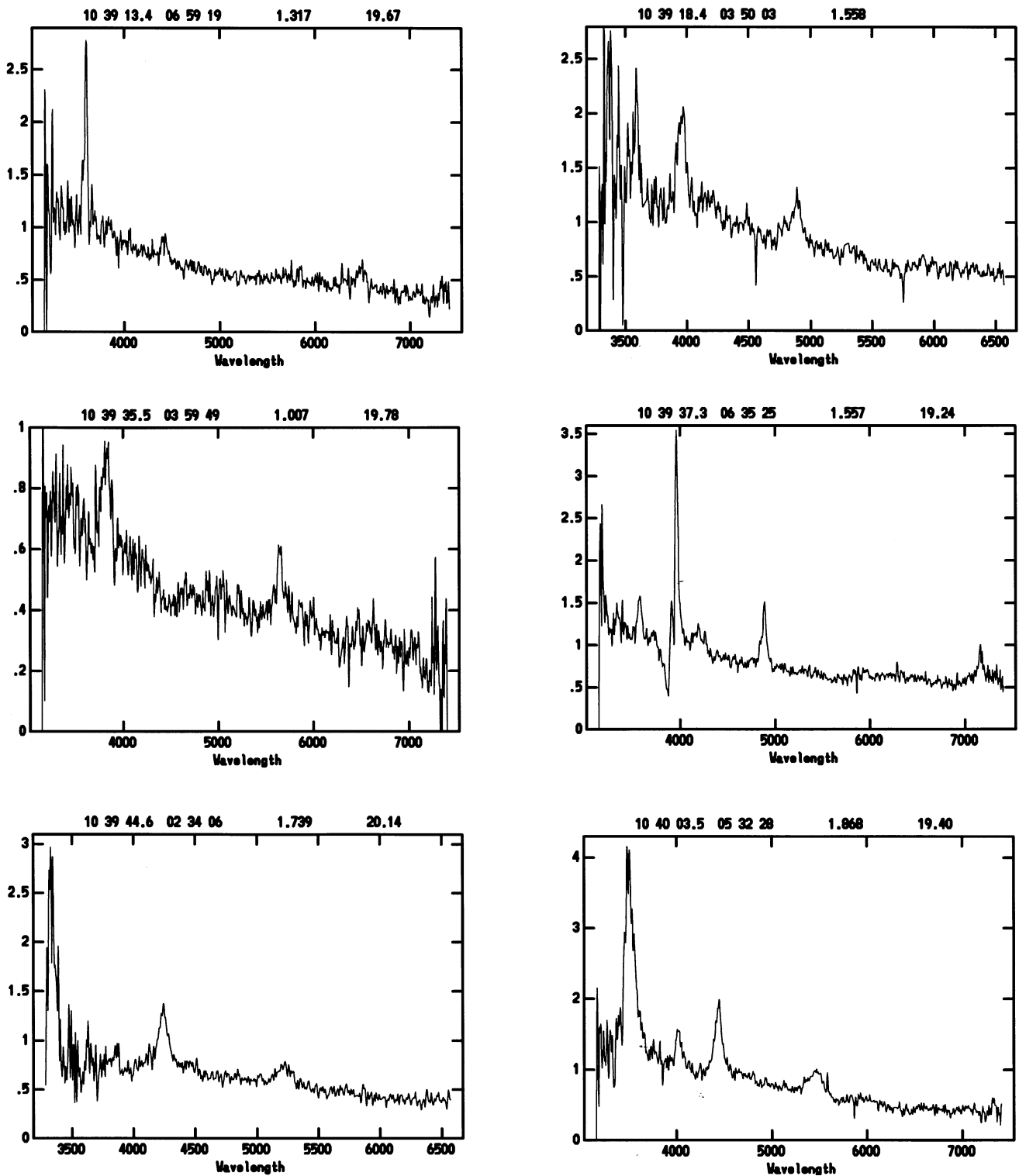


Figure 1 – continued

and one that is less distinct at  $4411.8 \text{ \AA}$ . These correspond to redshifts of 1.923 and 1.848. With the (imprecise) emission redshift of 1.997, the outflow speeds for these two troughs are  $v/c \sim 0.025$  ( $7500 \text{ km s}^{-1}$ ) and  $v/c \sim 0.051$  ( $15280 \text{ km s}^{-1}$ ).

**10 36 00.4 06 45 26.** Absorption lines at  $4465.3$  and  $3574.4 \text{ \AA}$  are identified with C IV and N V at redshift 1.883. Although

moderately wide, these lines are not BAL troughs. A weaker line at  $4019.2 \text{ \AA}$  gives redshift 1.871, if identified with Si IV + O IV. The absorption lines cause the emission redshift of 1.899 to be imprecise.

**10 37 03.7 07 04 27.** This appears to be a BAL quasar. There is a trough shortward of C IV at  $4811.2 \text{ \AA}$ , which corresponds to



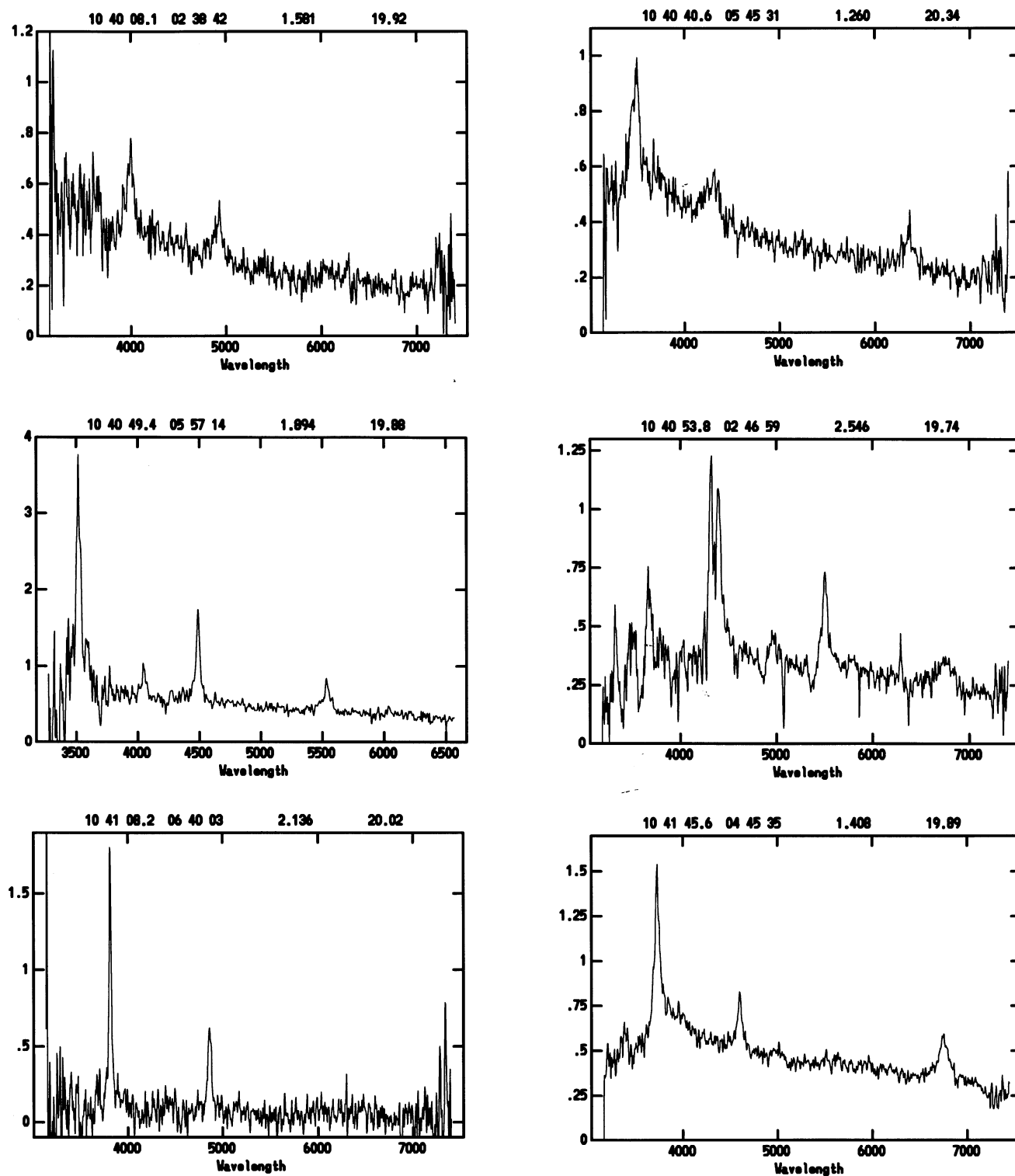


Figure 1 – continued

redshift 2.106. With the emission redshift of 2.341, the outflow speed is  $v/c \sim 0.073$  ( $21\,800\text{ km s}^{-1}$ ). There is a further trough at  $3846.9\text{ \AA}$ , which, if identified with Nv, corresponds to redshift 2.102. Further absorption appears to be present shortward of this trough.

**10 38 13.2 04 32 13.** This appears to be a BAL quasar. There is

a trough shortward of C iv that is resolved into (at least three) components at  $3995.4$ ,  $3937.6$  and  $3881.1\text{ \AA}$ . The central redshift is 1.542. With the (imprecise) emission redshift of 1.587, the central outflow speed is  $v/c \sim 0.018$  ( $5300\text{ km s}^{-1}$ ).

**10 39 13.4 06 59 19.** Narrow emission lines, especially C iv.

**10 39 37.3 06 35 25.** This is a BAL quasar. There is a trough

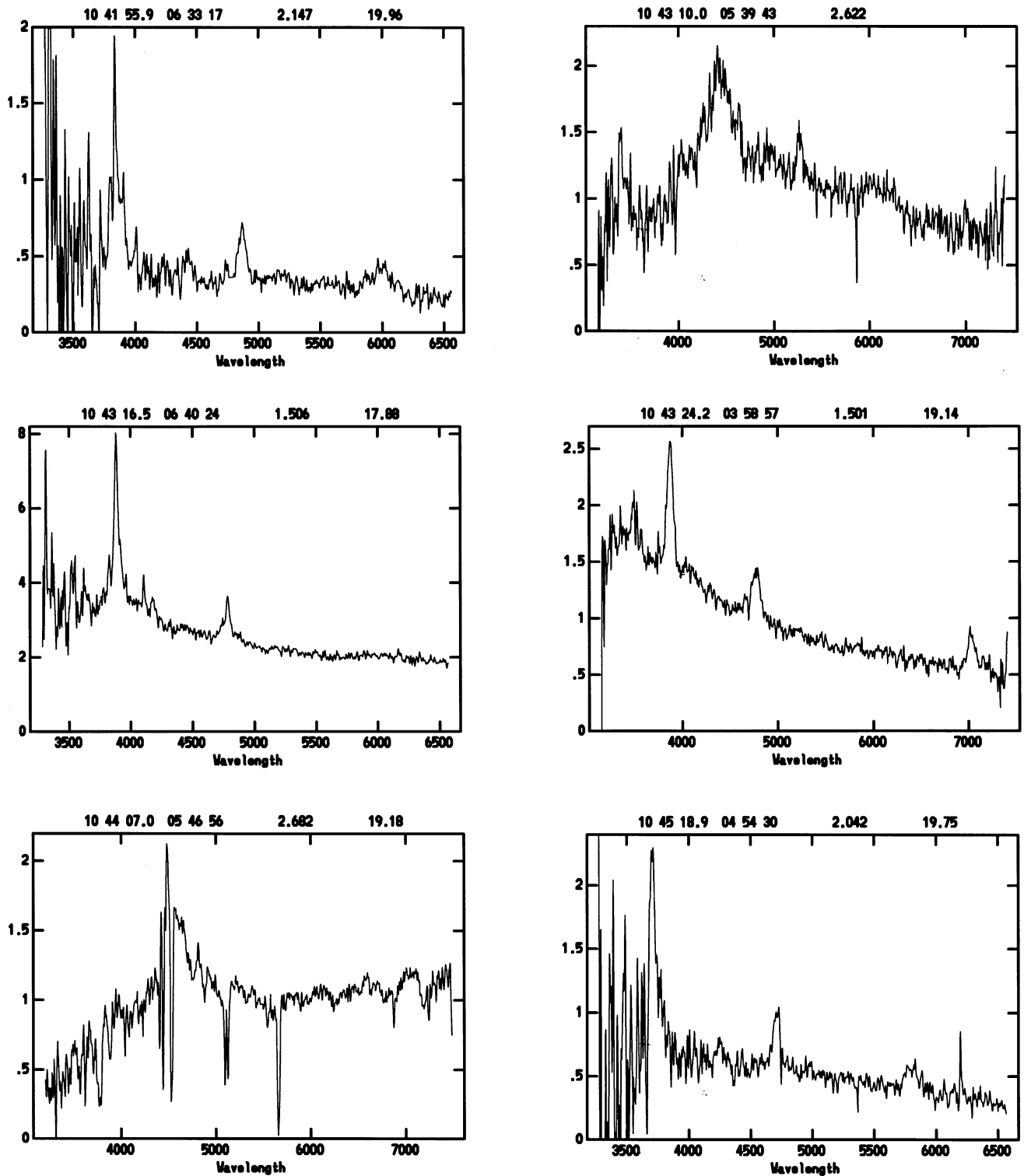


Figure 1 – continued

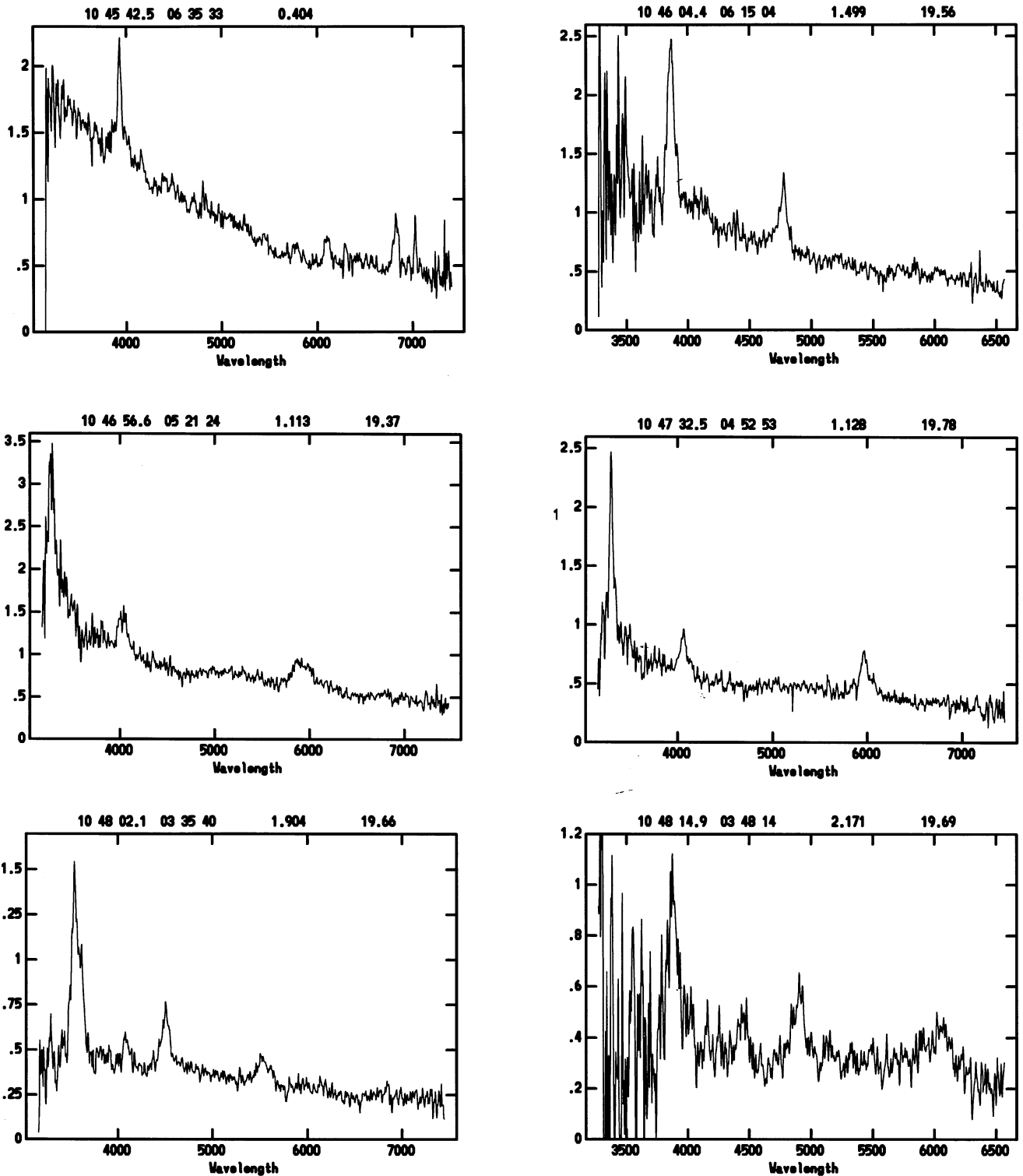
shortward of C IV at 3875.9 Å, which corresponds to redshift 1.502. With the emission redshift of 1.557, the outflow speed is  $v/c \sim 0.022$  (6500 km s<sup>-1</sup>). There is also narrow C IV absorption at 3936.1 Å. The emission lines are narrow.

**10 40 53.8 02 46 59.** This a BAL quasar. There are three troughs that correspond to the same system: C IV at 5365.7 Å; Si IV + O IV at 4852.8 Å; O VI at 3588.5 Å. The mean redshift of these is 2.467.

With the emission redshift of 2.546, the outflow speed is  $v/c \sim 0.023$  (6800 km s<sup>-1</sup>). Narrow absorption lines are also present in the spectrum.

**10 41 08.2 06 40 03.** Narrow emission lines.

**10 43 10.0 05 39 43.** This is an unusual quasar. There are apparently real emission lines at 4403.9 and 5263.5 Å, plus a more doubtful line at 3388.8 Å. However, no redshift fits even a pair of

Figure 1 – *continued*

these lines well. We have therefore assumed that the strong, broad line at  $4403.9 \text{ \AA}$  corresponds to  $\text{Ly}\alpha$  and deduced  $z = 2.622$ ; this redshift could be entirely wrong. Note the striking similarity of the spectrum of this quasar to that of the very unusual quasar 10 44 07.0 05 46 56 ( $z = 2.682$ ). There are absorption lines at  $5865.4, 5599.0, 5444.4, 4189.4,$  and  $3969.3 \text{ \AA}$ .

**10 44 07.0 05 46 56.** This is a very unusual quasar, having

strong, broad  $\text{Ly}\alpha + \text{Nv}$  emission, but no  $\text{CIV}$  emission. Note that, in Table 2, the equivalent width of the  $\text{Ly}\alpha + \text{Nv}$  emission is rather uncertain because of the difficulty in defining the continuum reliably. There is a strong associated absorption system:  $5656.6, 5122.4, 5091.4, 4530.1, 4440.1$  and  $3776.4 \text{ \AA}$ , corresponding to  $\text{CIV}, \text{OIV}, \text{SiIV}, \text{NV}, \text{Ly}\alpha$  and  $\text{OVI}$  at mean redshift 2.652. With the emission redshift of 2.682, the outflow

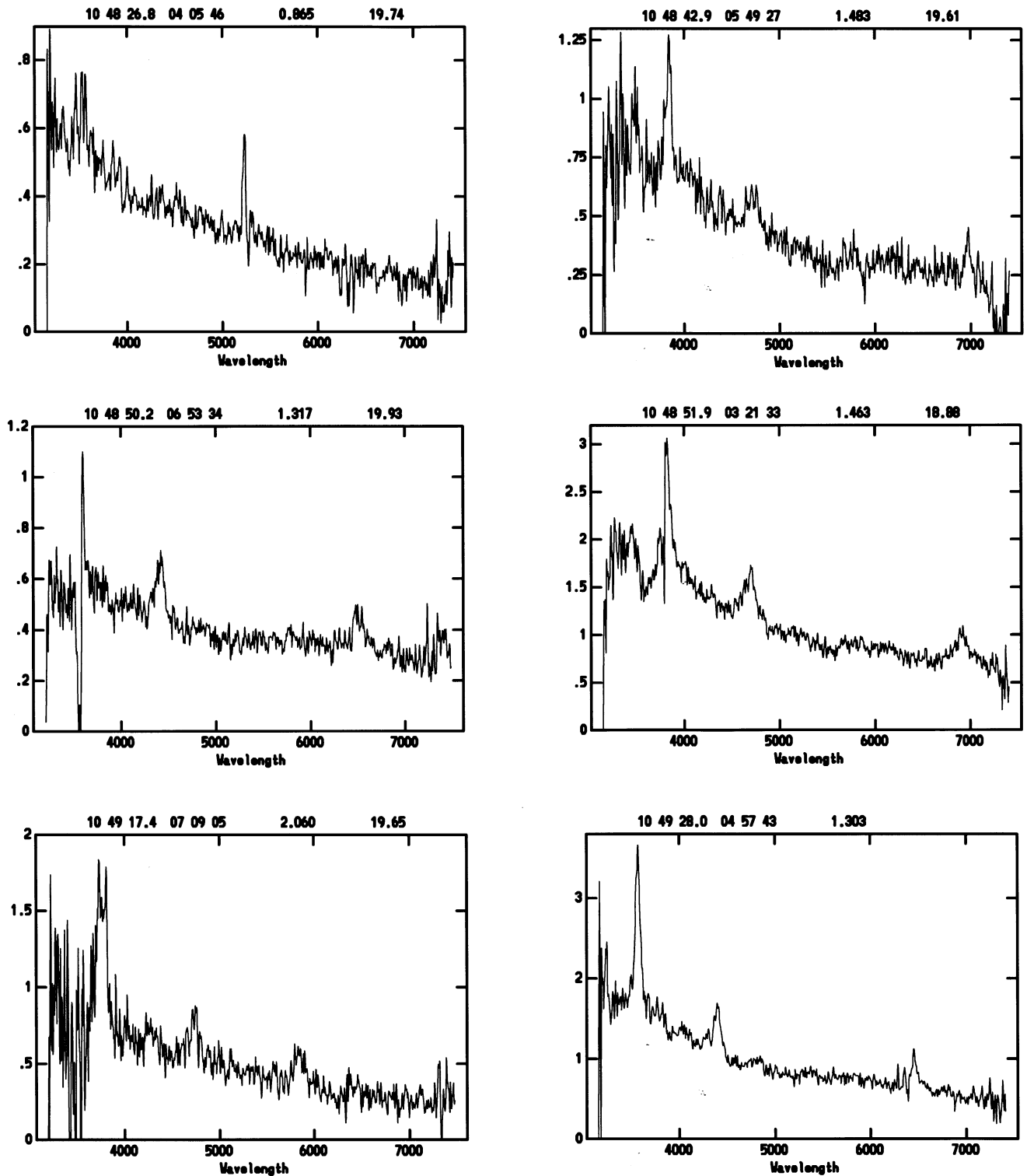


Figure 1 – continued

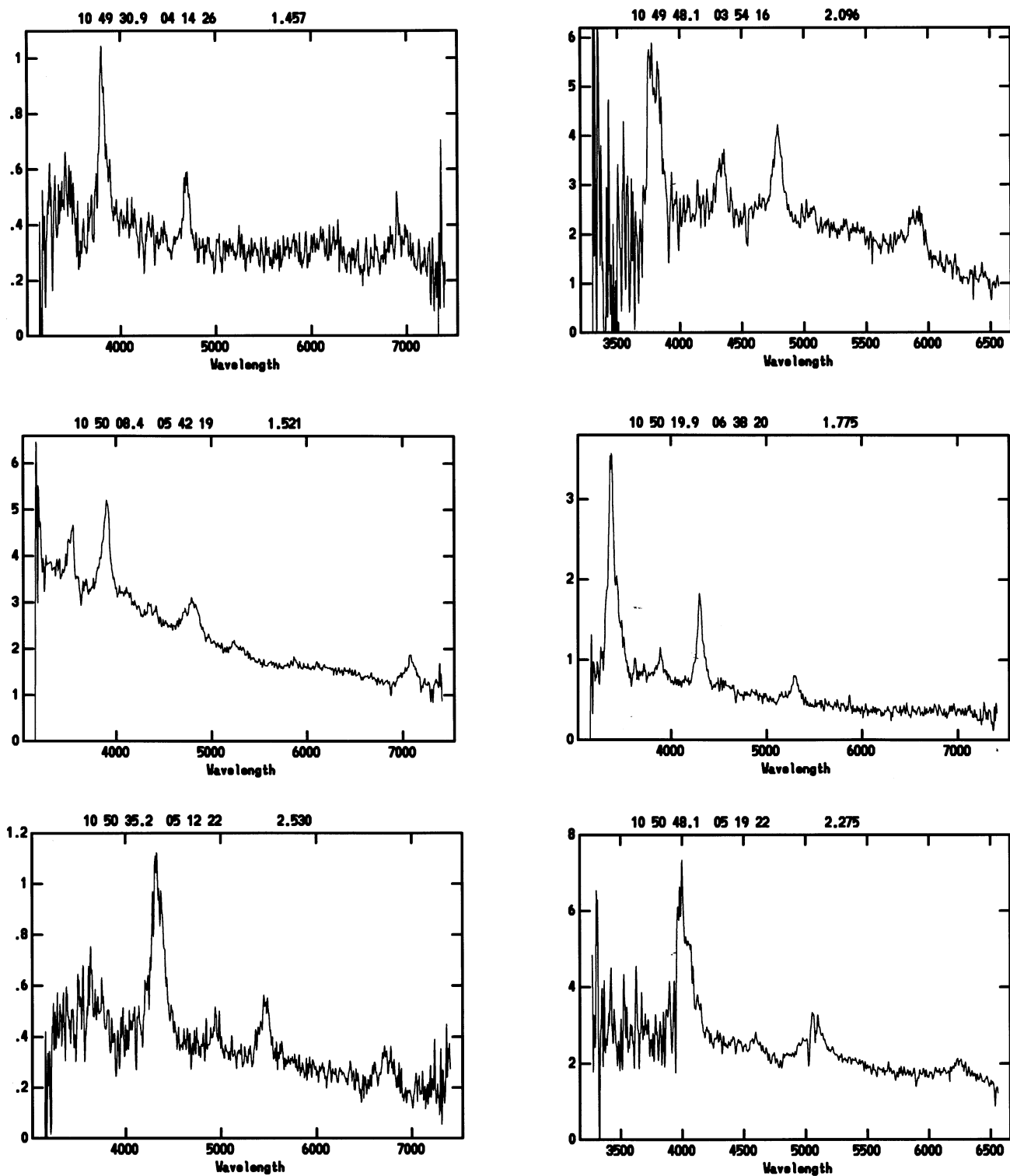
speed is  $v/c \sim 0.008$  ( $2400 \text{ km s}^{-1}$ ). Other absorption lines appear to be present at  $7241.1$ ,  $7186.5$ ,  $4879.0$ ,  $4754.4$ ,  $4402.6$ ,  $4227.8$ ,  $4038.7$ ,  $3880.6$ ,  $3618.2$ , and  $3566.1 \text{ \AA}$ . See Campusano & Clowes (1995) for further discussion of this quasar. Note the similarity of the spectrum to that of 10 43 10.0 05 39 43.

**10 48 50.2 06 53 34.** This is a BAL quasar. There is a trough shortward of C IV at  $3550.5 \text{ \AA}$ , which corresponds to redshift

$1.292$ . With the emission redshift of  $1.317$ , the outflow speed is  $v/c \sim 0.011$  ( $3250 \text{ km s}^{-1}$ ).

**10 48 51.9 03 21 33.** This is a BAL quasar. There is a trough shortward of C IV at  $3576.0 \text{ \AA}$ , which corresponds to redshift  $1.309$ . With the emission redshift of  $1.463$ , the outflow speed is  $v/c \sim 0.064$  ( $19340 \text{ km s}^{-1}$ ).

**10 49 48.1 03 54 16.** An absorption line at  $4541.1 \text{ \AA}$  is

Figure 1 – *continued*

presumably C IV at redshift 1.932. The (imprecise) emission redshift is 2.096. Although moderately wide (FWHM  $\sim 20 \text{ \AA}$ ), the absorption line is not a BAL trough.

**10 50 08.4 05 42 19.** An absorption line at  $3632.0 \text{ \AA}$  is presumably C IV at redshift 1.345. The (imprecise) emission

redshift is 1.521. Although moderately wide (FWHM  $\sim 28 \text{ \AA}$ ), the absorption line is not a BAL trough.

**10 50 48.1 05 19 22.** There are narrow absorption lines at (at least)  $5075.2, 5021.9, 3941.1$  and  $3912.3 \text{ \AA}$ , and possibly a broader absorption at  $4783.8 \text{ \AA}$ . The line at  $5021.9$  is presumably C IV at

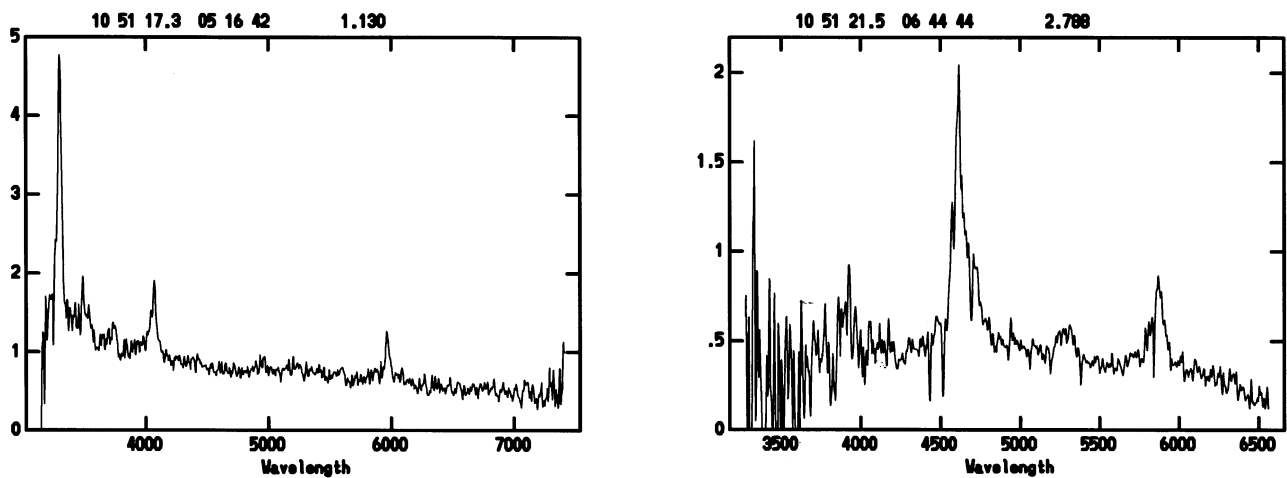


Figure 1 – continued

redshift 2.242, which corresponds to  $\text{Ly}\alpha$  at 3912.3. The (imprecise) emission redshift is 2.275.

**10 51 21.5 06 44 44.** Absorption at (at least) 5841.6, 5379.0, 5190.1, 5057.2, 4922.1, 4843.0, 4693.4, 4583.9, 4514.1, 4434.2 Å.

#### 4 THE LARGE QUASAR GROUP

The observations presented here conclude the follow-up of this AQD sample of quasars. The 62 survey quasars from this paper and the 56 survey quasars presented by Clowes & Campusano (1994) constitute a total sample of 118 quasars (71 per cent of the candidates), across a continuous area of  $\sim 25.3 \text{ deg}^2$ , and to a limiting magnitude of  $B_J \sim 20$ . The sample was defined, by computer selection, to be spatially unbiased and thus suitable for the analysis of structure in the early Universe. Note that there are few such surveys, combining uniform, wide-angle coverage and a faint limiting magnitude. LQGs, such as the Clowes & Campusano (1991) LQG that was found in this sample, would most probably escape detection in surveys of different design (e.g. pencil-beam or narrow-strip surveys).

We give here a brief summary of the present observational status of the Clowes & Campusano LQG (see also Clowes et al. 1995), following the observations presented above and also some other related observations that are in preparation for publication. Formal analyses will be given elsewhere (e.g. Campusano et al., in preparation).

Fig. 2 shows the positions on the sky of the quasars with  $1.2 \leq z < 1.4$ , corresponding to the large quasar group (LQG, Clowes & Campusano 1991) in field 927 (lower half) and field 999 (upper half). The observations in field 999 are from a northern extension of our AQD survey (Graham et al., in preparation). The LQG is readily apparent. Note that we have so far confirmed 118 quasars in field 927 and 52 in field 999. To make the two halves of the figure comparable, readers may imagine two more quasars with  $1.2 \leq z < 1.4$  to be scattered in the upper half. Note that in the lower half we have continued to include the three (spatially unbiased) quasars that are not from our survey (see Clowes & Campusano 1991).

The LQG has also been confirmed in an independent survey – the Chile–UK Quasar Survey (CUQS; Newman et al. 1998; Newman, in preparation). The CUQS was created because the

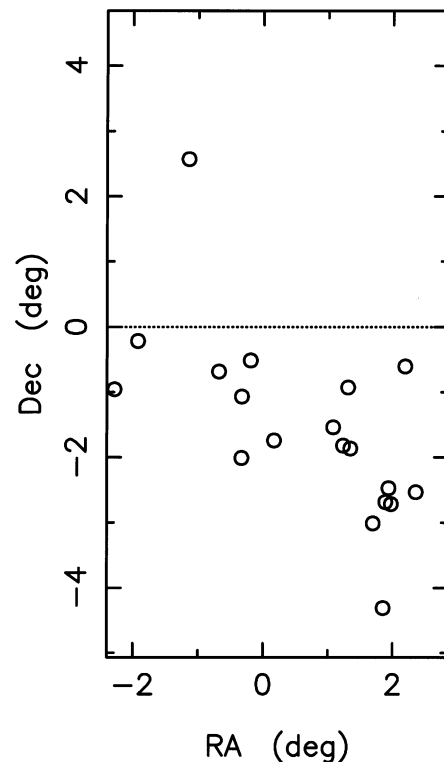


**Figure 2.** The positions on the sky of the quasars with  $1.2 \leq z < 1.4$ , corresponding to the large quasar group (LQG, Clowes & Campusano 1991) in field 927 (lower half) and field 999 (upper half). Note that there are, in total, nearly 2.5 times as many confirmed quasars in field 927 as in field 999. In field 927, the figure shows the 15 members of the LQG from our survey and three more not from our survey. The units are degrees.

LQG strikes the boundaries of the AQD survey. When completed, the CUQS will cover an area of at least  $100 \text{ deg}^2$  centred on the LQG, together with a control area of at least  $40 \text{ deg}^2$  elsewhere. It uses the ultraviolet-excess method for selection and the fibre spectrograph (two-degree field) of the Las Campanas 2.5-m Du Pont Telescope for spectroscopic confirmation. The limiting magnitude of the CUQS is currently brighter than that of the AQD survey. Thus some members are lost from the CUQS, but the LQG nevertheless appears as a highly significant structure.

**ACKNOWLEDGMENTS**

LEC was funded partly by grant 1970/735 from the Fondo Nacional de Desarrollo Científico y Tecnológico, Chile. The spectroscopic observations were obtained at the CTIO 4-m telescope, with the help of the night assistants Mauricio Fernández, Manuel Hernández and Hernán Tirado. The data were processed with IRAF, partly at CTIO and partly at the Universidad de Chile. Analysis of the data at the Universidad de Chile and in the UK used the facilities of the Centro de Procesamiento Digital de Imágenes (CPDI) and Starlink respectively. Cerro Tololo Inter-American Observatory is operated by the Association of Universities for Research in Astronomy, Inc. (AURA), under contract with the National Science Foundation. IRAF is distributed by the National Optical Astronomy Observatories, which is operated by AURA, Inc., under cooperative agreement with the National Science Foundation.

**REFERENCES**

- Campusano L. E., Clowes R. G., 1995, in Meylan G., ed., Proceedings of the ESO Workshop, QSO Absorption Lines. Springer, Berlin, p. 247  
 Clowes R. G., 1986, *Mitt. Astron. Ges.*, 67, 174  
 Clowes R. G., Campusano L. E., 1991, *MNRAS*, 249, 218  
 Clowes R. G., Campusano L. E., 1994, *MNRAS*, 266, 317  
 Clowes R. G., Cooke J. A., Beard S. M., 1984, *MNRAS*, 207, 99  
 Clowes R.G., Campusano L. E., Graham M. J., 1995, in Maddox S. J., Aragón-Salamanca A., eds, *The 35th Herstmonceux Conference, Wide Field Spectroscopy and the Distant Universe*. World Scientific Publishing, Singapore, p. 400  
 Keable C. J., 1987, PhD thesis, Univ. Edinburgh  
 Newman P. R., Clowes R. G., Campusano L. E., Graham M. J., 1998, in Colombi S., Mellier Y., Raban B., eds, *14th IAP Colloquium, Wide Field Surveys in Cosmology*. Editions Frontières, p. 408  
 Stone R. P. S., Baldwin J. A., 1983, *MNRAS*, 204, 347
- This paper has been typeset from a  $\TeX/\LaTeX$  file prepared by the author.